A study of the T2 defect and the emission properties of the E3 deep level in annealed melt grown ZnO single crystals

W. Mtangi,[1] M. Schmidt,[1] F. D. Auret,[1] W. E. Meyer,[1] P. J. Janse van Rensburg,[1] M. Diale,[1] J. M. Nel,[1] A. G. M. Das,[2] F. C. C. Ling,[3] and A. Chawanda[4]
[1]*Department of Physics, University of Pretoria, Private Bag X20, Hatfield 0028, South Africa*
[2]*School of Information Technology, Monash South Africa, Roodepoort 1725, South Africa*
[3]*Department of Physics, University of Hong Kong, Pokfulam Road, Hong Kong*
[4]*Department of Physics, Midlands State University, P. Bag 9055, Senga Road, Gweru, Zimbabwe*

(Received 2 November 2012; accepted 7 March 2013; published online 22 March 2013)

We report on the space charge spectroscopy studies performed on thermally treated melt-grown single crystal ZnO. The samples were annealed in different ambients at 700 °C and also in oxygen ambient at different temperatures. A shallow donor with a thermal activation enthalpy of 27 meV was observed in the as-received samples by capacitance-temperature, CT scans. After annealing the samples, an increase in the shallow donor concentrations was observed. For the annealed samples, E27 could not be detected and a new shallow donor with a thermal activation enthalpy of 35 meV was detected. For samples annealed above 650 °C, an increase in acceptor concentration was observed which affected the low temperature capacitance. Deep level transient spectroscopy revealed the presence of five deep level defects, E1, E2, E3, E4, and E5 in the as-received samples. Annealing of the samples at 650 °C removes the E4 and E5 deep level defects, while E2 also anneals-out at temperatures above 800 °C. After annealing at 700 °C, the T2 deep level defect was observed in all other ambient conditions except in Ar. The emission properties of the E3 deep level defect are observed to change with increase in annealing temperature beyond 800 °C. For samples annealed beyond 800 °C, a decrease in activation enthalpy with increase in annealing temperature has been observed which suggests an enhanced thermal ionization rate of E3 with annealing. © *2013 American Institute of Physics*. [http://dx.doi.org/10.1063/1.4796139]

I. INTRODUCTION

ZnO is a wide and direct bandgap semiconductor with a high exciton binding energy, high saturation velocity, high electron mobility, and excellent resistance to radiation damage. The latter feature of the material qualifies it for the fabrication of devices that can operate in high radiant conditions, e.g., in outer space applications and reactor laboratories. Since in space applications, devices are usually subjected to very harsh temperature conditions, it is a requirement for the material to be resistant to high temperature annealing effects for better operating efficiency and lifetime of devices. This is because annealing tends to modify the operation of devices by inducing defects, recovering/activating the neutral dopants, increasing the concentration of shallow donors[1,2] resulting in surface conduction,[3] and at times annealing out defects. For devices operating in the UV region, the problem arises when defects induced in the material due to high temperature exposure are optically active. Optical absorption by these defects will influence efficient operation of devices.

Considering the low oxygen and nitrogen partial pressures as well as the high temperatures which a detector on a space craft is exposed to, there is a need to have knowledge of the defects that can be introduced at high temperatures under different ambient conditions. Studies on the annealing induced defects in ZnO have been performed using deep level transient spectroscopy (DLTS) techniques in which deep level defects have been observed. It has also been demonstrated that at some particular temperatures, formation of these deep level defects is ambient related. Quemener *et al.*[4] have investigated the effects of annealing hydrothermally grown ZnO samples at 1100 °C in Ar, O_2, and Zn. Their results have revealed the introduction of E2 whose formation strongly depends on the ambient used. Mtangi *et al.*[5] also investigated the effects of annealing melt grown single crystals at 300 °C in Ar, O_2, and H_2 and they have revealed the introduction of E4 in Ar and H_2 ambient. Annealing ZnO at 1100 °C in Zn vapour and Ti has been performed by Weber and Lynn.[6] Selim *et al.*[7] have also investigated the effects of annealing ZnO under Zn-rich conditions and reported a red colouration of ZnO which has been attributed to O_v, while Ehret and Greenstone[8] have also reported the changes in the colour of red ZnO upon heat treatment at different temperatures, a hint which points out to the deep level defects that are formed at those temperatures. Clearly, the effects of thermal treatment have an effect on the optical and electronic properties of ZnO.

Schmidt *et al.*[9] have demonstrated the photo-ionisation of a defect level T2 observed in Pulsed Laser deposited grown ZnO samples using optical deep level transient spectroscopy (ODLTS) while Ellguth *et al.*[10] showed the photo-ionisation of the T2 and E4 defects in PLD ZnO thin films also using ODLTS. Such observation has not been reported in bulk single crystal ZnO and neither has T2 been observed in as-grown Cermet single crystal ZnO. Current literature indicates that the T2 has only been observed in polycrystalline ZnO, thin films, and also in vapour phase grown material used by Frank *et al.*[11] Ye *et al.*[12] have reported a defect with

 © 2013 American Institute of Physics

Downloaded 15 May 2013 to 147.8.230.100. This article is copyrighted as indicated in the abstract. Reuse of AIP content is subject to the terms at: http://jap.aip.org/about/rights_and_permissions

the same activation enthalpy as T2 after O-implantation and subsequent annealing of melt grown ZnO samples in air, while Mtangi *et al.*[13] reported a defect they labelled Ex with a similar activation enthalpy to that of T2 after annealing melt grown single crystal ZnO samples at 700 °C in Ar + O_2. It must be noted that the material used by Ye *et al.*[12] and Mtangi *et al.*[13] was obtained from the same supplier. Frank *et al.*[11] also demonstrates that the E4 is optically active and is a negative-U centre. Therefore, the existence of the T2/Ex and E4 defects in ZnO crystals will definitely affect device operation within the UV region.

Also of interest in ZnO defect studies is a defect labelled E3. This defect has been observed to be present in all ZnO crystals in very high concentrations regardless of material growth technique. The study of this defect and its identity is an interesting topic as it is not clear where it originates from as yet. Research performed on ZnO, however, has the vast majority of reports assigning it to an oxygen vacancy related defect,[14–16] while other reports suggest it to be a transition metal ion related defect.[17,18] Debate about the identity of E3 is still raging. With the difficulty in growing reproducible p-type ZnO, knowing the identity of E3 and its behaviour, i.e., in terms of its annealing behaviour can be essential as this might assist in controlling material doping. It has since been observed that the conditions under which T2 and E4 are introduced reduce the intensity of the E3 peak.[13]

Using the capacitance based DLTS technique, under dark conditions, it has been observed from the DLTS spectra that E3 has a peak height which increases with increase in rate window frequency as has been reported by,[12,19] an indication that it has a temperature activated capture cross-section. However, its capture barrier energy has not been obtained yet as its capture process seems not to follow a simple exponential process. It was also suggested that the electron capture rate for the E3 level is not constant during the filling pulse as it depends on the occupancy of the defect and the available carriers for electron capture.[19]

In this paper, we perform a further investigation on the introduction of T2/Ex in ZnO under various annealing conditions and the effects of high temperature oxygen annealing on it using the conventional DLTS measurement techniques. We also report, for the first time, on the observed change in emission properties and activation enthalpy of the E3 defect with changes in annealing temperature.

II. EXPERIMENT

Melt grown single crystal ZnO samples obtained from Cermet Inc. with a batch number K3-1553-01 AV were used in this study. Six samples were cut from the same 1 cm^2 wafer. The as-received sample was used as the reference sample for this experiment. The rest of the samples were then annealed at 700 °C for 1 h in different ambient conditions. Before annealing, the samples were ultrasonically cleaned in methanol for 5 min and blow dried using nitrogen gas. For Ar + O_2 annealing, a set of two samples was first annealed in Ar. One of the samples was then removed from the furnace. The remaining sample was then annealed for another 1 h in O_2 ambient. For the O_2 + Ar annealing, a set of two samples was also used. First the two samples were annealed in O_2, after which one of the samples was removed. The remaining sample was annealed in Ar ambient for another 1 h. Vacuum annealing was performed at a pressure of approximately 1×10^{-6} Torr. For annealing involving Ar and O_2, a controlled flow of gas of 3.0 l/min was used. For samples annealed in O_2 ambient at different temperatures, a 1 cm^2 wafer from the same batch of samples as in the latter case was used. All annealing was performed prior to Schottky and ohmic contact fabrication. Prior to contact fabrication, all samples were cleaned as outlined by Mtangi *et al.*[13] Pd Schottky contacts of diameter 0.5 mm and thickness 50 nm were fabricated on the Zn-polar face while ohmic contacts of Al/Au with thicknesses of 30/50 nm were fabricated on the O-polar face of the samples. Contact fabrication was done using the resistive evaporation system at a pressure of approximately 1×10^{-6} Torr.

III. RESULTS AND DISCUSSIONS

From the IV characteristics of the Schottky contacts fabricated on the ZnO samples used in this study, ideality factors of 1.09–1.40 were calculated. This indicates that pure thermionic emission proved to be the dominant current transport mechanism at room temperature. The as-received sample showed a leakage current in the order of 10^{-9} A at a reverse bias of 2.0 V and a series resistance in the order of 600 Ω. For the annealed samples, the oxygen annealed samples produced contacts with the least leakage current values in the order of 10^{-10} A at a reverse bias of 2.0 V and series resistance values in the order of 3 kΩ, while the vacuum annealed samples gave contacts with high leakage currents, in the order of 10^{-6} A at 2.0 V and series resistance values which are lower than those obtained in the as-received samples. Barrier heights of 0.82 eV were measured on the contacts fabricated on the oxygen annealed samples, while lower barrier heights of 0.66 eV were measured for the vacuum annealed samples. All the contacts fabricated were suitable for use in space charge spectroscopic techniques.

A. Shallow donors

We have investigated the effects of annealing on the shallow donors and the net doping concentration of the samples using capacitance temperature (C-T) scans and capacitance-voltage (C-V) measurements (van Opdorp's method[20]), respectively. In Figure 1(a), the net-doping concentration of the samples annealed at 700 °C in different ambients is presented. From the net doping profiles presented in Figure 1(a), we observed that the net doping concentration increases for all the annealed samples. In ambients with low oxygen partial pressures (Ar and vacuum), the net doping concentration is higher within a depth of 0.10 μm below the interface compared to that of the as-received sample.

For the samples annealed in oxygen ambient at different temperatures (Figure 1(b)), the net doping concentration for all the annealed samples is observed to increase as compared to that of the as-received samples. This increase is observed to be highly pronounced towards the surface. At a depth of 0.10 μm below the interface, an increase in net doping density

Downloaded 15 May 2013 to 147.8.230.100. This article is copyrighted as indicated in the abstract. Reuse of AIP content is subject to the terms at: http://jap.aip.org/about/rights_and_permissions

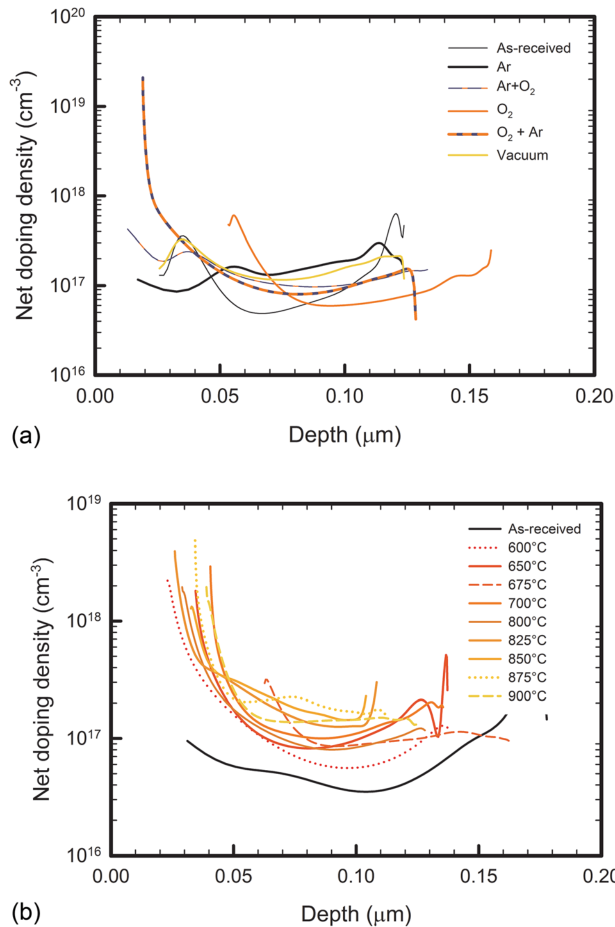

FIG. 1. Net doping density profiles of ZnO samples annealed in different ambient conditions at 700 °C. These profiles were recorded at room temperature and at a frequency of 50 kHz. Figure 1(b) Net doping density profiles of ZnO samples annealed in oxygen ambient at different temperatures. These profiles were recorded at room temperature and at a frequency of 50 kHz.

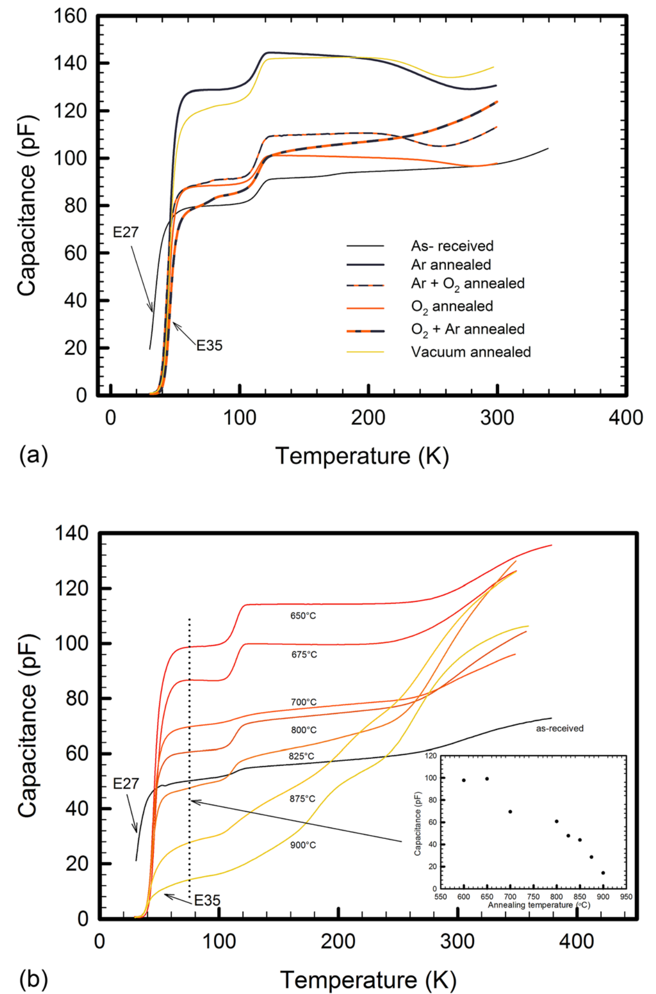

FIG. 2. Capacitance temperature scans for ZnO samples annealed in different ambient conditions at a temperature of 700 °C. These were recorded at a reverse bias of 2.0 V scanning up in temperature. Figure 2(b) Capacitance temperature scans for ZnO samples annealed in oxygen ambient at different temperatures. These scans were recorded at a reverse bias of 2.0 V scanning up in temperature. The inset shows the variation of capacitance with annealing temperature at 75 K.

with annealing is observed up to a temperature of 675 °C, after annealing at 700 °C and 800 °C, there is a decrease in the net doping density. An increase in net doping density is again noticed after annealing between 825 °C–875 °C and a decrease is observed after annealing at 900 °C. The C-T measurements in Figure 2(b) can be used to explain this trend, since the C-V measurements were performed at 300 K, where a fluctuation in the capacitance values is also observed. This fluctuation can be attributed to the partial contribution of the E3 level to the capacitance at this temperature which influences the determination of the net doping concentration. For samples annealed above 650 °C, this effect is crucial since the slope in the C-T characteristics at 300 K is very steep.

For the C-T scans presented in Figure 2, only in the as-grown samples, a shallow donor previously labelled E27 (Ref. 1) with an activation enthalpy of approximately 27 meV was observed. This donor has previously been attributed to the Zn_i.[1,2] In the annealed samples, E27 could not be detected and a shallow donor with an activation enthalpy of 35 meV was observed instead. There are two possibilities explaining the absence of the E27 in the annealed samples: (i) Either it was annealed-out as was also suggested by Mtangi *et al.*,[2] or (ii) There is an increase in the acceptor concentration with annealing, which in turn affects the position of the Fermi level. In the latter case, the lowering of the Fermi level would call for an increase in the degree of acceptor compensation within the annealed material. E27 would then be ionized at all temperatures and, therefore, it will not be observed by space charge spectroscopic techniques. With the lowering of the Fermi level, its electrons in the conduction band will easily be taken up by the acceptor states. The failure to observe the E27 in the annealed samples is also in agreement with what was theoretically suggested by Janotti and Van de Walle[21] and experimentally by Neuvonen *et al.*[22] that the Zn_i is highly mobile at temperatures around 600 °C and is not likely to be a stable donor.

The concentration of E35 is increased for the Ar and vacuum annealed samples (Figure 2(a)). This increase in the E35 concentration can be related to low oxygen partial pressure. For the oxygen annealed samples, E35 has the highest concentration in the sample annealed at 650 °C. Annealing at temperatures higher than 650 °C results in a decrease in the low temperature capacitance (Figure 2(b)). This decrease in capacitance witnessed for high temperature annealed

Downloaded 15 May 2013 to 147.8.230.100. This article is copyrighted as indicated in the abstract. Reuse of AIP content is subject to the terms at: http://jap.aip.org/about/rights_and_permissions

samples could be due to the increase in acceptor concentration with annealing temperature. The low temperature capacitance values show a pronounced trend with increase in annealing temperature (inset of Figure 2(b)). The inset shows the variation of capacitance with temperature at 75 K. The capacitance increases with increase in annealing temperature and reaches a maximum at an annealing temperature of 650 °C, after which it decreases with increase in annealing temperature.

B. Deep level defects

DLTS measurements performed on the un-annealed sample reveals the presence of five deep level defects (E1, E2, E3, E4, and E5) (Figure 3). Arrhenius plots of these deep level defects are presented in Figure 4. The activation enthalpies and apparent capture cross-sections of these defects are presented in Tables I and II. The E4 and E5 deep levels are being observed for the first time in the as-received samples

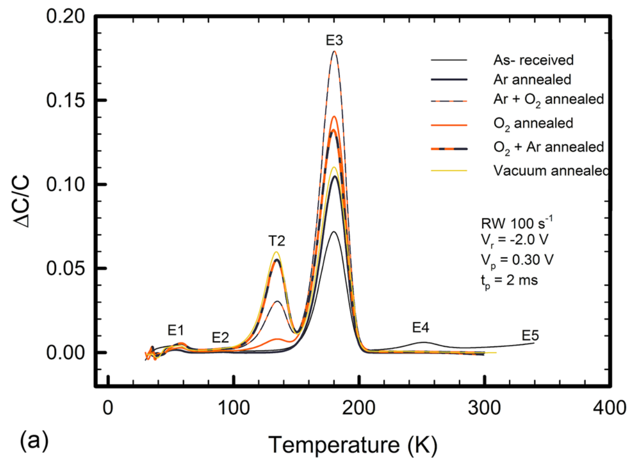

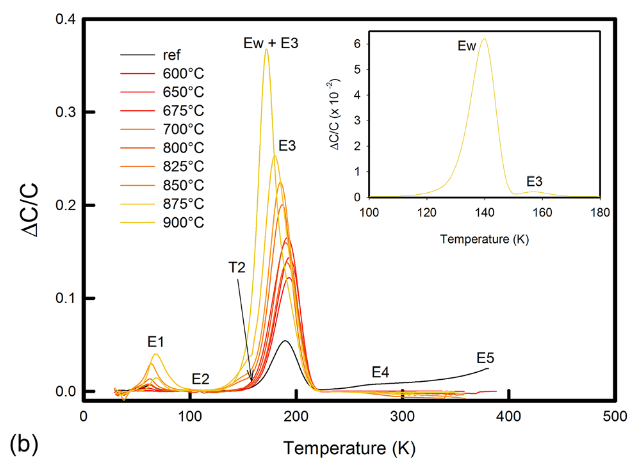

FIG. 3. Normalized DLTS spectra obtained from Pd/ZnO Schottky contacts for ZnO samples annealed at 700 °C in different ambient conditions. The spectra were recorded at a rate window frequency of 100 Hz, reverse bias voltage of 2.0 V, filling pulse of 0.3 V into forward bias and pulse width of 2.0 ms. Figure 3(b) Normalized DLTS spectra obtained from Pd/ZnO Schottky contacts for ZnO samples annealed in oxygen ambient at different temperatures. The spectra were recorded at a rate window frequency of 500 Hz, reverse bias voltage of 2.0 V, filling pulse of 0.4 V into forward bias and pulse width of 2.0 ms. The inset shows the spectra obtained from the 900 °C annealed samples at a rate window frequency of 5 Hz.

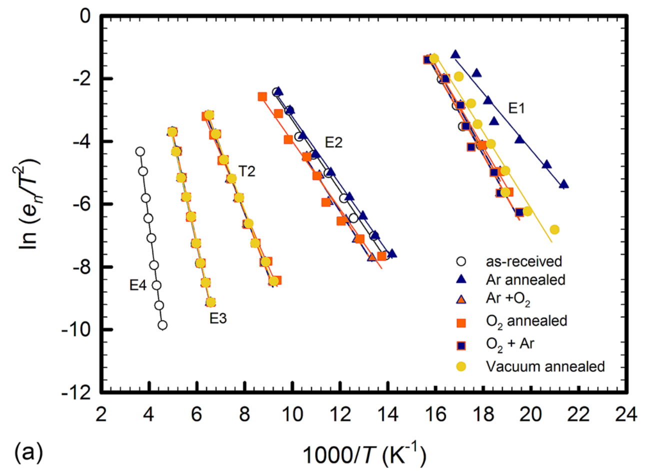

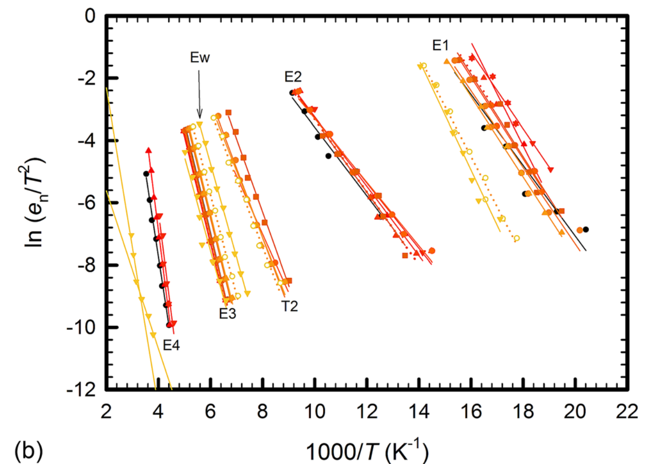

FIG. 4. Arrhenius plots obtained from the ZnO samples annealed in different ambient conditions at 700 °C to calculate the activation enthalpy and apparent capture cross-section of the observed defects. Figure 4(b) Arrhenius plots obtained from the ZnO samples annealed at different temperatures in oxygen ambient to calculate the activation enthalpy and apparent capture cross-section of the observed defects.

from Cermet. Since we have not observed the E4 and E5 in as-received samples before,[13,18,19,23] we attribute these defects to sample growth conditions. A defect with an activation enthalpy similar to the one we have measured has been observed by Frank *et al.*[11] in vapour phase grown ZnO which they attributed to an oxygen vacancy. Since our E4 defect compares very well to the E4 by Frank *et al.*[11] in both activation enthalpy and capture cross-section, we can assign our E4 defect to the O-vacancy. Assignment of E4 to the oxygen vacancy in this case implies that there is a high possibility this particular batch of samples was grown under non-equilibrium conditions, i.e., low oxygen partial pressures. The activation enthalpy and apparent capture cross-section of E5 have been obtained as 1.05 eV and 5×10^{-12} cm^2, respectively.

Interesting enough, annealing samples in different ambient conditions at 700 °C anneal out the E4 and E5 deep level defects. For samples annealed in oxygen ambient at different temperatures (Figure 3(b)), below an annealing temperature of 675 °C, E5 is annealed out, but E4 is still present. After annealing at 675 °C, both the E4 and E5 defects anneal-out. Above the 800 °C annealing temperature, the E2 defect

Downloaded 15 May 2013 to 147.8.230.100. This article is copyrighted as indicated in the abstract. Reuse of AIP content is subject to the terms at: http://jap.aip.org/about/rights_and_permissions

TABLE I. Values of activation enthalpy and apparent capture cross-section for defects observed in samples annealed in different ambient conditions at 700 °C as obtained from standard Arrhenius analysis.

	E1[a]		E2		T2		E3		E4	
Annealing ambient	Activation enthalpy (meV)	Capture X-section (cm^2)	Activation enthalpy (meV)	Capture X-section (cm^2)	Activation enthalpy (meV)	Capture X-section (cm^2)	Activation enthalpy (meV)	Capture X-section (cm^2)	Activation enthalpy (meV)	Capture X-section (cm^2)
As-received	113	3×10^{-13}	97	4×10^{-18}			301	1×10^{-15}	523	7×10^{-14}
Ar	78	2×10^{-15}	93	3×10^{-18}			293	7×10^{-16}		
$Ar + O_2$	117	9×10^{-13}	102	4×10^{-18}	167	2×10^{-17}	295	8×10^{-16}		
O_2	112	3×10^{-13}	93	1×10^{-18}	153	5×10^{-18}	296	9×10^{-16}		
$O_2 + Ar$	117	7×10^{-13}			174	3×10^{-17}	297	1×10^{-15}		
Vacuum	105	1×10^{-13}			170	2×10^{-17}	289	6×10^{-16}		

[a]Note must be taken on the variation and assignment of the activation enthalpies to the E1 deep level as it is not clear whether it is the same defect in the annealed samples as it is in the as-received samples.

anneals-out. Within these annealing temperatures, the peak position of the E1 defect is observed to shift to higher temperatures for all rate window frequencies, implying that the emission rate of the E1 defect decreases for samples annealed at high temperatures. The activation enthalpy of E1 is also observed to increase with increase in annealing temperature.

C. Introduction of T2

Annealing ZnO crystals at 700 °C in vacuum and oxygen ambient introduces the T2 deep level defect, while argon annealing does not introduce the T2 deep level defect (Figure 3(a)). Making a follow up of this observation, one might be tempted to assume that oxygen annealing followed by argon annealing might anneal out the T2 level. We have further performed a test to see if this assumption could be valid by annealing a sample that was first annealed in O_2 in Ar ambient ($O_2 + Ar$) and also the one annealed first in Ar and then in O_2 ($Ar + O_2$). Results from this particular experiment reveal the introduction of T2 in the $Ar + O_2$ situation, while an increase in intensity of T2 has been observed in the $O_2 + Ar$ annealed samples. A defect with a similar activation enthalpy to T2 has been observed by Ye *et al.*[12] in O-implanted melt-grown single crystal ZnO samples annealed in air and Schmidt *et al.*[9] in PLD grown ZnO thin films. This defect was explained as an intrinsic defect but the microscopic origins of this defect were not disclosed[12] Quemener *et al.*[4] also observed a defect E2 with an activation enthalpy and capture cross-section which are almost similar to that of T2 in hydrothermal grown ZnO annealed in oxygen and argon but not in Zn. They attributed the origins of this defect to be impurity related. Since this defect (E2/T2) has been observed in material grown using different techniques; and proves to be ambient related (promoted mainly under vacuum in melt-grown [this work] and O_2 ambient in hydrothermally grown[4]), there is a chance that this defect is intrinsic to the ZnO material.

In all the annealing ambients used, vacuum annealing introduces the T2 level in very high concentrations, an indication that might suggest formation of this defect favours low oxygen partial pressures. Such a trend of an increase in

TABLE II. Values of activation enthalpy and apparent capture cross-section for defects observed in samples annealed at different temperatures in oxygen ambient as obtained from standard Arrhenius analysis.

	E1[a]		E2		T2		Ew		E3		E4	
Annealing temperature (°C)	Activation enthalpy (meV)	Capture X-section (cm^2)	Activation enthalpy (meV)	Capture X-section (cm^2)	Activation enthalpy (meV)	Capture X-section (cm^2)	Activation enthalpy (meV)	Capture X-section (cm^2)	Activation enthalpy (meV)	Capture X-section (cm^2)	Activation enthalpy (meV)	Capture X-section (cm^2)
As-received	98	7.7×10^{-15}	95	2.1×10^{-18}					306	2.1×10^{-15}	473	1.8×10^{-15}
600	144	1.9×10^{-10}	91	1.8×10^{-18}					296	7.4×10^{-16}	576	5.0×10^{-13}
650	106	1.3×10^{-13}	96	3.4×10^{-18}					303	1.2×10^{-15}	572	7.6×10^{-13}
675	113	2.5×10^{-13}	101	5.4×10^{-18}					301	1.2×10^{-15}		
700	113	2.1×10^{-13}	88	1.3×10^{-18}	161	3.5×10^{-18}			301	1.3×10^{-15}		
800	114	2.8×10^{-13}	100	5.0×10^{-18}	202	3.2×10^{-16}			304	1.7×10^{-15}		
825	106	3.9×10^{-14}			193	5.9×10^{-17}			294	1.4×10^{-15}		
850	111	8.5×10^{-14}			184	2.5×10^{-17}			293	1.5×10^{-15}		
875	139	2.1×10^{-12}			189	2.9×10^{-17}			278	9.9×10^{-16}		
900	152	2.0×10^{-10}					259	7.3×10^{-16}	261	5.1×10^{-17}	442 219	3.4×10^{-18} 7.1×10^{-22}

[a]Note must be taken on the variation and assignment of the activation enthalpies to the E1 deep level as it is not clear whether it is the same defect in the annealed samples as it is in the as-received samples.

Downloaded 15 May 2013 to 147.8.230.100. This article is copyrighted as indicated in the abstract. Reuse of AIP content is subject to the terms at: http://jap.aip.org/about/rights_and_permissions

T2 concentration with decrease in oxygen partial pressure has been observed by Schmidt *et al*.[9] in PLD ZnO thin films. However, drawing such a conclusion at this point could be premature as Ar ambient annealing does not support this argument. An extensive investigation on the effects of Ar annealing on ZnO by varying the annealing temperature needs to be performed.

Since the intensity of T2 is very low in all the annealed samples compared to that of E3, it was difficult to resolve the T2 and E3 peaks using the DLTS techniques. The DLTS peak which contains E3 is a superposition of T2 and E3 defects. We have separated the E3 DLTS peak from the T2 peak by simulating the E3 defect and subtracting it from the peak that contains E3 and T2. This simulation has been performed by making use of the fact that DLTS is a superposition of peaks with different emission rates. The simulation that was used is contained in Appendix A. Figure 5 shows the DLTS spectra of E3 and T2 defects plotted from experimentally obtained data and simulated data for the 700 °C O_2 annealed samples. It can be clearly observed that the T2 and E3 are distinct deep level defects. The estimated activation enthalpy of T2 ranges from 153 meV to 202 meV (Tables I and II); with the lower activation enthalpies being obtained from samples in which the normalized DLTS intensity of T2 is high (Figure 1(a)) and the high activation enthalpies being obtained from samples in which the normalized DLTS intensity is low as has also been observed by Schmidt *et al*.[9]

Having observed the T2 level in samples annealed at 700 °C,[13] when the E4 and E5 have annealed out, we have performed an investigation to establish the temperature at which the T2 level is introduced. This was done in oxygen ambient with varying temperatures. Up to an annealing temperature of 675 °C, the T2 deep level is not induced. Beyond this annealing temperature, T2 is induced. Increasing the annealing temperature causes an increase in the concentration of T2 up to an annealing temperature of 875 °C. At 900 °C, it is not clear whether T2 is still present or has been annealed out (Figure 3(b)). In both sets of experiments, it has been observed that for low activation enthalpies of T2, the apparent capture cross-sections are also low (Tables I and II). After 900 °C annealing, a new defect labelled Ew is induced. It is not very clear whether T2 is annealed out or not. The high concentration of Ew makes it difficult to observe T2, i.e., if it is still present.

A concentration-depth profile of T2 for the 700 °C O_2 annealed samples is presented in Figure 6(a). This was calculated using the method highlighted in Appendix B. A constant bias variable pulse method was used to obtain this profile. A reverse bias of 2.0 V was used with a positive going filling pulse which was increased in steps of 0.1 V starting from −0.5 V and ending at 0.5 V. This profile indicates that the occupancy of the T2 level linearly decreases as we move into the bulk of the semiconductor.

D. Emission properties of E3

The as-received ZnO samples contain the E3 deep level defect in very high concentrations. This defect has been observed in several ZnO samples grown using different

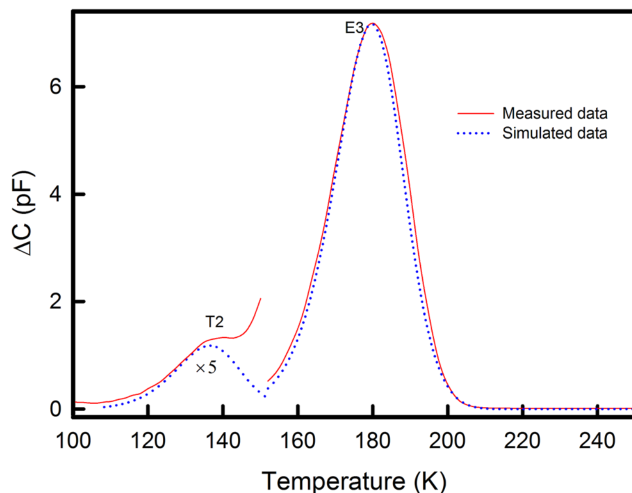

FIG. 5. Deconvolution of the DLTS spectra to separate the T2 and E3 defects using the method highlighted in Appendix B. The experimental data used were obtained from the 700 °C oxygen annealed samples.

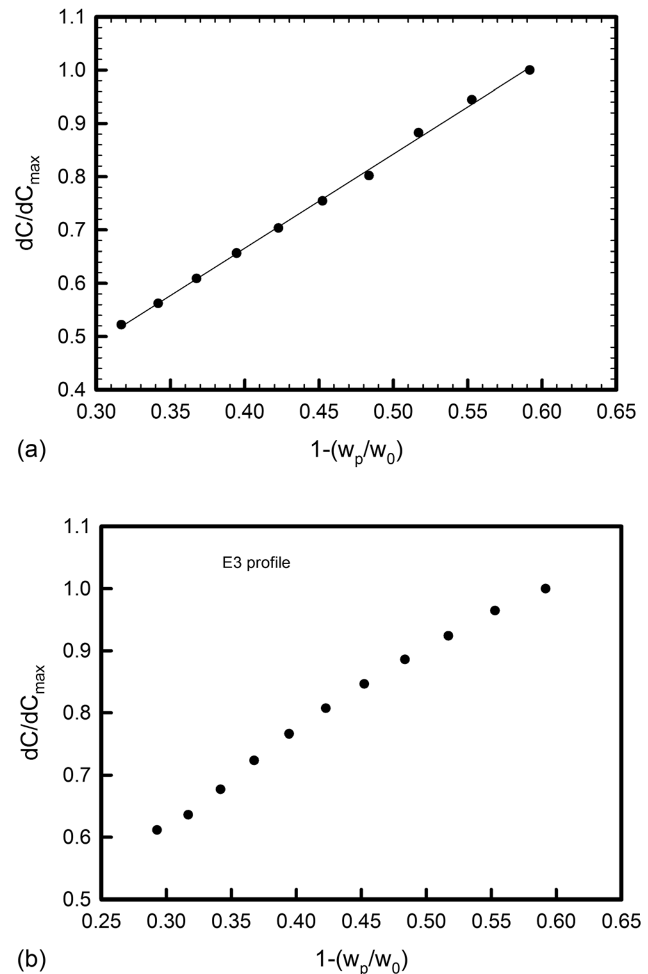

FIG. 6. Trap concentration depth profile of the T2 defect obtained from the 700 °C O_2 annealed ZnO samples using the fixed bias variable pulse technique. This profile was obtained at a reverse bias of 2.0 V with increasing filling pulse in steps of 0.1 V from −0.5 V to 0.5 V. Figure 6(b). Trap concentration depth profile of the E3 defect obtained from the 700 °C O_2 annealed ZnO samples using the fixed bias variable pulse technique. This profile was obtained at a reverse bias of 2.0 V with increasing filling pulse in steps of 0.1 V from −0.5 V to 0.5 V.

Downloaded 15 May 2013 to 147.8.230.100. This article is copyrighted as indicated in the abstract. Reuse of AIP content is subject to the terms at: http://jap.aip.org/about/rights_and_permissions

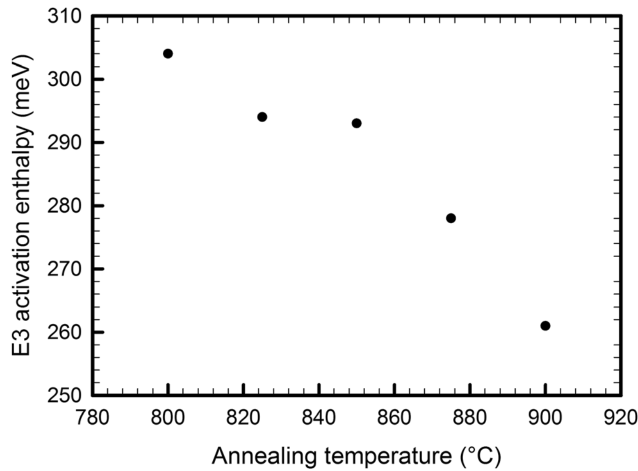

FIG. 7. Variation of the E3 activation enthalpy with increase in annealing temperature to illustrate changes in the thermal ionization of E3.

techniques.[14–18,24–27] However, the microscopic origins of this defect are not clear as yet. Annealing ZnO samples in different ambient increases the intensity of the DLTS peak for the E3 defect (Figure 3(a)), with the highest intensity being observed for the Ar + O_2 annealed samples. It must be noted that it is not clear whether the increase in the peak intensity of E3 stems from its high concentration or the lower sample capacitance for a frequency of 1 MHz at T = 150 K. There is an observed change in the activation enthalpy of the E3 defect for the annealed samples compared to that of the as-received samples. This gives a hint that annealing of ZnO at high temperatures affects the emission properties of the E3 defect. This effect has, however, not been reported before. A shift in the peak position of E3 for the same rate window frequency (Figure 3(b)) has been observed which also directly affects its activation enthalpy and capture cross-section for annealing temperatures above 800 °C. The thermal emission rate of E3 is observed to increase with an increase in annealing temperature. This implies that the thermal ionization rate of E3 is enhanced with increasing annealing temperature. Thus, for samples annealed at high temperatures, the activation enthalpy of E3 is reduced (Figure 7).

Figure 6(b) shows a concentration-depth profile of E3 for the 700 °C O_2 annealed sample which was calculated using the constant bias variable pulse technique illustrated in Appendix B. This profile indicates that E3 has a concentration gradient that increases towards the surface.

IV. CONCLUSIONS

As-received ZnO samples contain the E27 shallow donor. After annealing, the E27 shallow donor could not be detected. This could possibly be due to the fact that it is annealed-out or it is always readily ionized at all the measurement temperatures. A new shallow donor, E35 is observed in all the annealed samples. Oxygen annealing introduces donors and acceptors in ZnO. Above annealing temperatures of 800 °C, acceptors are introduced in high concentrations compared to donors resulting in high compensation of the material which affects the low temperature capacitance. As-received ZnO samples contain five deep level defects as determined using DLTS techniques. The E4 and E5 defects are observed to anneal out at temperatures above 650 °C, but in O_2 ambient, E4 is reintroduced after 900 °C annealing. In O_2 ambient, E2 anneals-out at temperatures above 800 °C. Above annealing temperatures of 825 °C in O_2 ambient, the activation enthalpy of E1 increases with increasing annealing temperature. T2 is introduced in ZnO after annealing melt grown single crystals at 700 °C. High concentrations of T2 are obtained after annealing samples in ambients with low O_2 partial pressures. Ar atmosphere, however, suppresses the formation of T2 in the samples used in this study. 900 °C O_2 annealing introduces a new defect Ew with an activation enthalpy of 259 meV from standard Arrhenius analysis that has not been reported before. E3 shows an enhanced thermal ionization rate with increase in annealing temperature where its activation enthalpy decreases with increase in annealing temperature above 800 °C.

ACKNOWLEDGMENTS

The authors wish to thank the University of Pretoria for the financial support. Matthias Schmidt was funded by the Postdoctoral Fellowship Program of the University of Pretoria. This work is based upon research supported by the National Research Foundation (NRF). Any opinion, findings and conclusions or recommendations expressed in this material are those of the author(s) and therefore the NRF does not accept any liability in regard thereto. The Laplace DLTS software and hardware used in the research was kindly provided by A. R. Peaker (Centre for electronic Materials Devices and Nanostructures, University of Manchester) and L. Dobaczewski (Institute of Physics, Polish Academy of Sciences).

APPENDIX A: DECONVOLUTION OF THE E3 AND T2 DEEP LEVELS

For $N_t \ll N_{net}$, DLTS is a superposition of peaks with different emission rates which can be given by a function, f,

$$f = \sum_i a_i[1 - \exp(-e_n t_{rw})], \tag{A1}$$

where a_i is a coefficient that relates to the defect concentration, e_n is the thermal emission rate, t_{rw} is the rate window which relates to the gate times such that the DLTS signal is in our case calculated from

$$S(T) = \frac{1}{2t_{rw}} \int_{\lambda}^{t_{rw}} a_i[1 - \exp(-e_n t_{rw})] de_n t - \int_{t_{rw}}^{2t_{rw}-\lambda} a_i[1 - \exp(-e_n t_{rw})] de_n t, \tag{A2}$$

where λ defines the dead time for the capacitance transient. If E3 can be simulated and the result is subtracted from the superimposed spectrum, then T2 can be evaluated for all the samples annealed in different ambients independent of E3.

Downloaded 15 May 2013 to 147.8.230.100. This article is copyrighted as indicated in the abstract. Reuse of AIP content is subject to the terms at: http://jap.aip.org/about/rights_and_permissions

APPENDIX B: CALCULATION OF THE DEFECT DEPTH PROFILE

The maximum width of the depletion region is proportional to the applied reverse voltage as[21]

$$w_0 \propto \sqrt{-V_r + V_{bi}}, \tag{B1}$$

where w_0 is the depletion region width with no pulse applied, V_r is the reverse bias voltage, V_{bi} is the built in potential. For a given filling pulse height, the width of the depletion region which contains the filled traps can be calculated from $w_0 - w_p$, where w_p is the depletion width after application of a pulse, given by

$$w_p \propto \sqrt{-V_p + V_{bi}}, \tag{B2}$$

where V_p is the filling pulse voltage. The ratio of the filled region to the entire depletion region width is given by

$$\frac{w_0 - w_p}{w_0} = 1 - \frac{w_p}{w_0} = 1 - \sqrt{\frac{-V_r + V_{bi}}{-V_p + V_{bi}}}. \tag{B3}$$

Variation of the filling pulse voltage will alter the occupancy of the depletion region and hence the measured peak height of the DLTS signals. A plot of the normalized DLTS signal against the ratio of filled depletion width to the entire width will give a profile of a defect.

[1] H. von Wenckstern, Ph.D. dissertation, Universität Leipzig, 2008.
[2] W. Mtangi, J. M. Nel, F. D. Auret, A. Chawanda, M. Diale, and C. Nyamhere, Physica B **407**, 1624 (2012).
[3] D. C. Look, Superlattices Microstruct. **42**, 284 (2007).
[4] V. Quemener, L. Vines, E. V. Monakhov, and B. G. Svensson, Appl. Phys. Lett. **100**, 112108 (2012).
[5] W. Mtangi, F. D. Auret, W. E. Meyer, M. J. Legodi, P. J. Janse van Rensburg, S. M. M. Coelho, M. Diale, and J. M. Nel, J. Appl. Phys. **111**, 094504 (2012).
[6] M. H. Weber and K. G. Lynn, J. Phys.: Conf. Ser. **262**, 012063 (2011).
[7] F. A. Selim, M. H. Weber, D. Solodovnikov, and K. G. Lynn, Phys. Rev. Lett. **99**, 085502 (2007).
[8] W. Ehret and A. Greenstone, J. Am. Chem. Soc. **65**, 872 (1943).
[9] M. Schmidt, M. Ellguth, R. Karsthof, H. v. Wenckstern, R. Pickenhain, M. Grundmann, G. Brauer, and C. C. Ling, Phys. Status Solidi B **249**, 588 (2012).
[10] M. Ellguth, M. Schmidt, R. Pickenhain, H. V. Wenckstern, and M. Grundmann, Phys. Status Solidi B **248**, 941 (2011).
[11] T. Frank, G. Pensl, R. T. Zaera, J. Zuniga-Perez, C. M. Tomas, V. M. Sanjose, T. Ohshima, H. Itoh, D. M. Hofmann, D. Pfisterer, J. Sann, and B. Meyer, Appl. Phys. A **88**, 141 (2007).
[12] Z. R. Ye, X. H. Lu, G. W. Ding, S. Fung, C. C. Ling, G. Brauer, and W. Anwand, Semicond. Sci. Technol. **26**, 095016 (2011).
[13] W. Mtangi, F. D. Auret, M. Diale, W. E. Meyer, A. Chawanda, H. de Meyer, P. J. Janse van Rensburg, and J. M. Nel, J. Appl. Phys. **111**, 084503 (2012).
[14] F. D. Auret, J. M. Nel, M. Hayes, L. Wu, W. Wesch, and E. Wendler, Superlattices Microstruct. **39**, 17 (2006).
[15] V. Quemener, L. Vines, E. V. Monakhov, and B. G. Svensson, Int. J. Appl. Ceram. Technol. **8**, 1017 (2011).
[16] J. C. Simpson and J. F. Cordaro, J. Appl. Phys. **63**, 1781 (1988).
[17] H. von Wenckstern, G. Biehne, M. Lorenz, M. Grundmann, F. D. Auret, W. E. Meyer, P. J. Janse van Rensburg, M. Hayes, and J. M. Nel, J. Korean Phys. Soc. **53**, 2861 (2008).
[18] W. Mtangi, F. D. Auret, P. J. Janse van Rensburg, S. M. M. Coelho, M. J. Legodi, J. M. Nel, W. E. Meyer, and A. Chawanda, J. Appl. Phys. **110**, 094504 (2011).
[19] W. Mtangi, M. Schmidt, P. J. Janse van Rensburg, W. E. Meyer, F. D. Auret, J. M. Nel, M. Diale, and A. Chawanda, "On the temperature dependence of the electron capture cross-section of the E3 deep level observed in single crystal ZnO," SAIP2012 Conference Proceedings (unpublished).
[20] C. van Opdorp, Solid-State Electron. **11**, 397 (1968).
[21] A. Janotti and C. G. Van de Walle, Phys. Rev. B. **76**, 165202 (2007).
[22] P. T. Neuvonen, L. Vines, B. G. Svensson, and A. Y. Kuznetsov, Phys. Rev. Lett. **110**, 015501 (2013).
[23] W. Mtangi, F. D. Auret, C. Nyamhere, P. J. Janse van Rensburg, M. Diale, and A. Chawanda, Physica B **404**, 1092 (2009).
[24] M. Grundmann, H. V. Wenckstern, R. Pickenhain, Th. Nobis, A. Rahm, and M. Lorenz, Superlattices Microstruct. **38**, 317 (2005).
[25] F. D. Auret, S. A. Goodman, M. Hayes, M. J. Legodi, H. A. van Laarhoven, and D. C. Look, Appl. Phys. Lett. **79**, 3074 (2001).
[26] H. von Wenckstern, R. Pickenhain, H. Schmidt, M. Brandt, G. Biehne, M. Lorenz, M. Grundmann, and G. Brauer, Appl. Phys. Lett. **89**, 092122 (2006).
[27] W. Schottky and E. Spenke, "Zur quantitativen Durchführung der Raumladungs-und Randschichttheorie der Kristallgleichrichter," Veröffentlichungen der Siemens AG **XVIII**, 225–291 (1939).

Downloaded 15 May 2013 to 147.8.230.100. This article is copyrighted as indicated in the abstract. Reuse of AIP content is subject to the terms at: http://jap.aip.org/about/rights_and_permissions